

FRACTURE GROWTH AND COMPARISON TO ANALYTICAL SOLUTION FOR AN IN-SITU HYDRAULIC FRACTURING (HF) EXPERIMENT

SCCER-SoE Annual Conference 13.-14. September 2018, Horw (LU)

Dutler, N., Valley B., Gischig V., Villiger L., Krietsch H., Doetsch J., Jalali MR., & Amann, F.



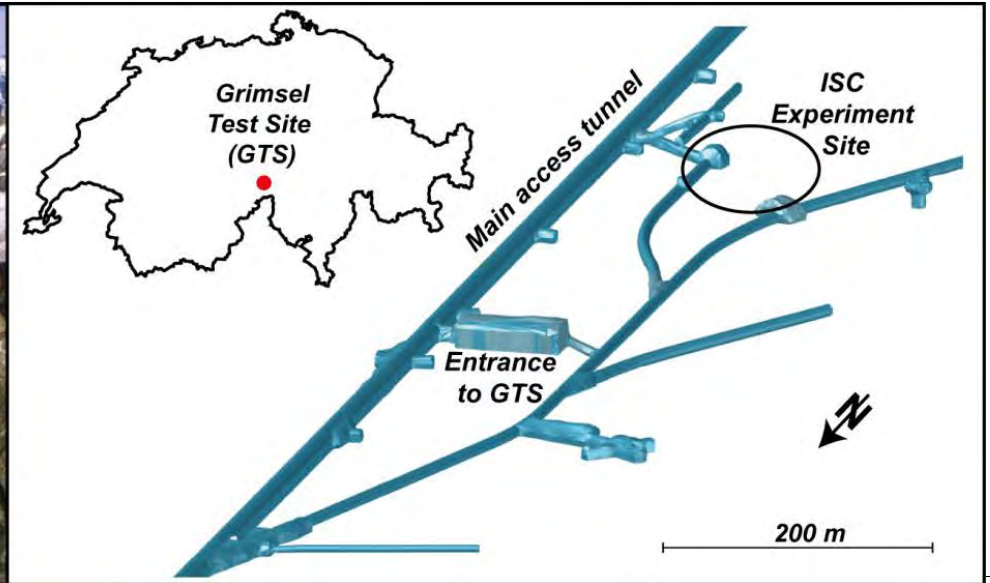
CONTENT

- Overview injection location and monitoring
- Seismic characteristics
- Overview of fracture growth
- Comparing fracture growth observations to analytical solutions

ISC - experiment

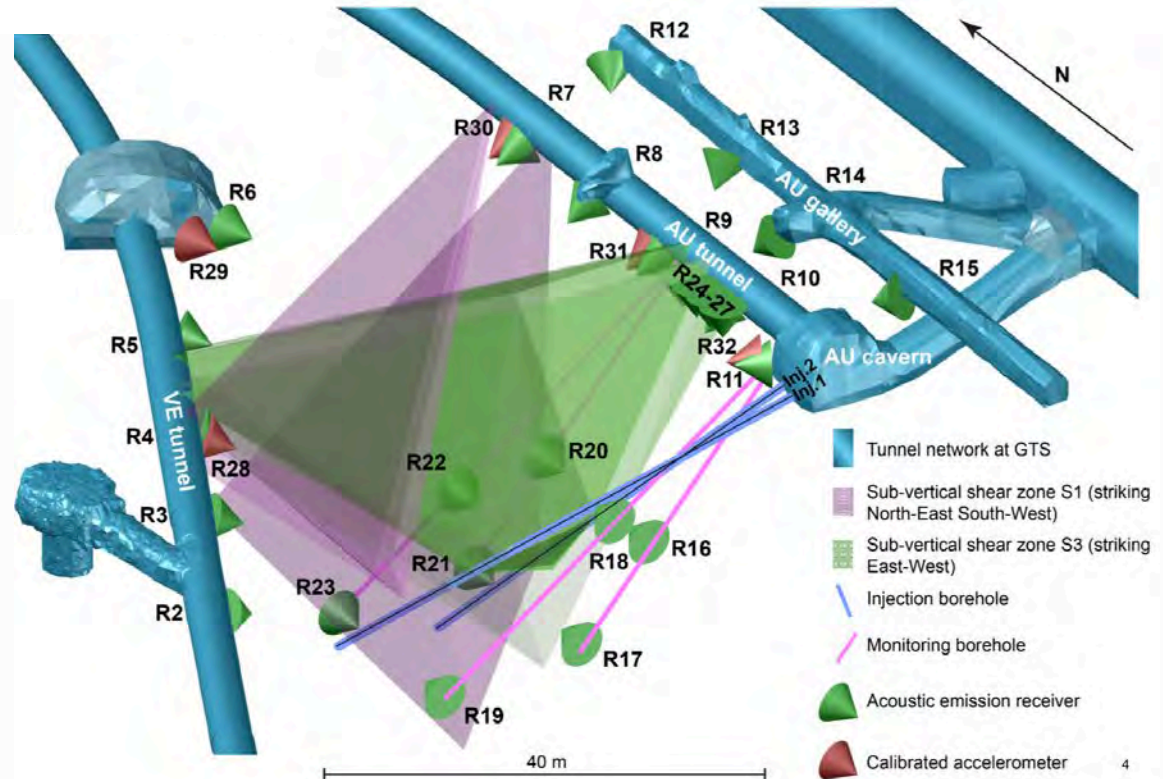
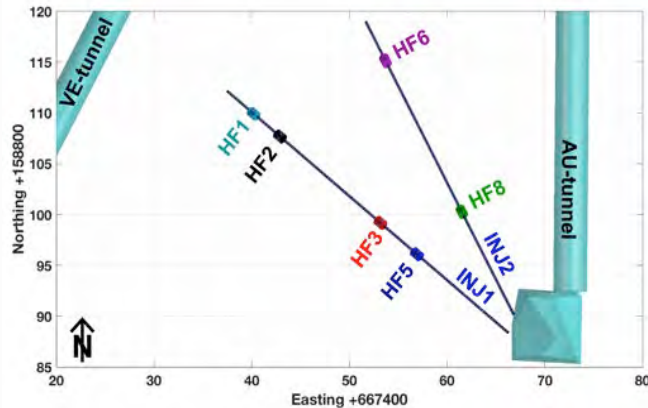
In-situ Stimulation and
Circulation experiment

More in Amann et al. (2018), SE9, 115



INJECTION LOCATIONS AND SEISMIC NETWORK

- 14 Piezo-electric acoustic emission receiver in tunnels
- 12 Piezos in monitoring boreholes
- 5 Calibrated Accelerometer



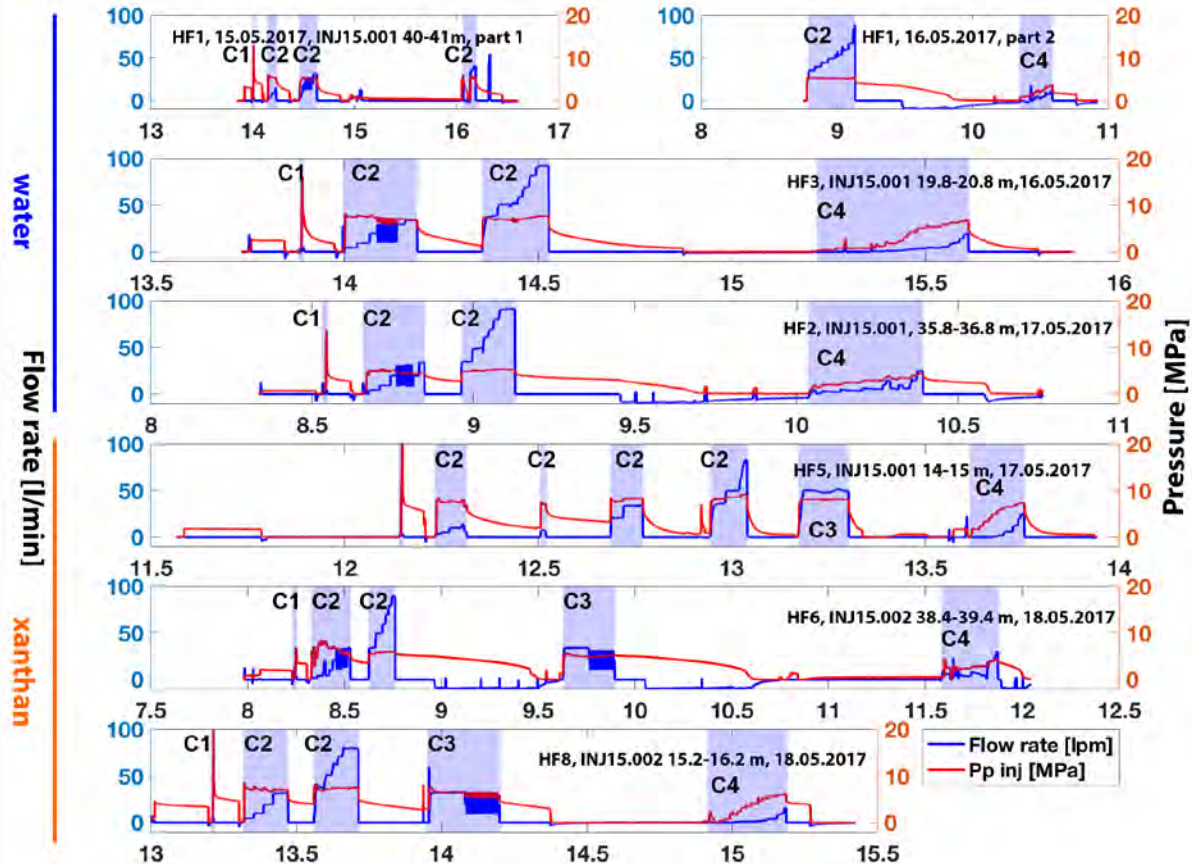
EXECUTED INJECTION PROTOCOL

Injection fluid:

- 3x water
- 3x xanthan-salt-water with 35 times higher viscosity (non-newtonian!) than water at a shear rate of 1 Hz
- In total: 1000 l per injection

Similar injection Protocol:

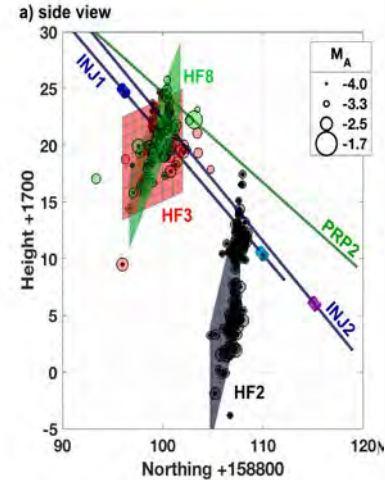
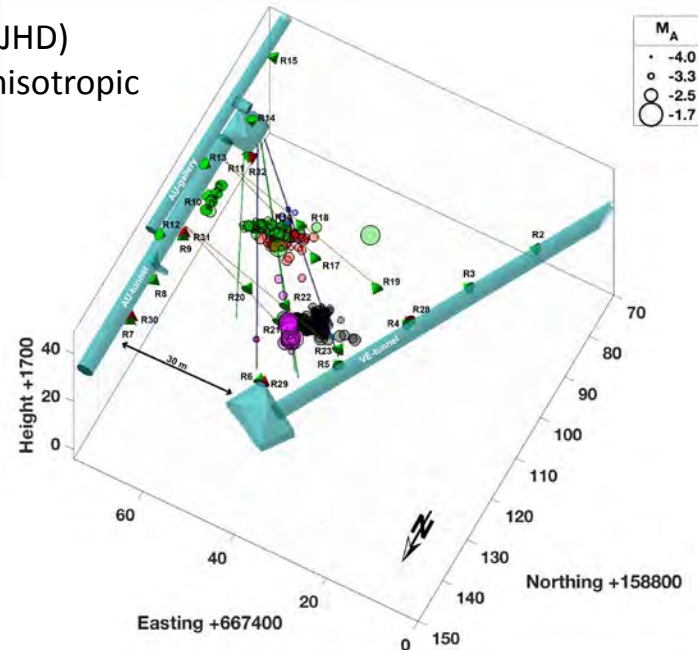
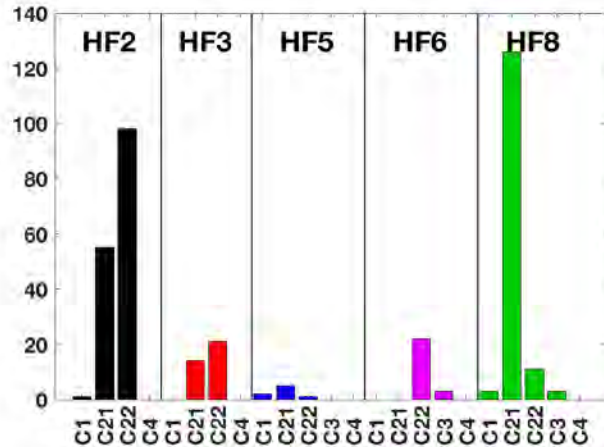
- C1** Break down cycle
- C2** Fracture propagation cycle
- C3** Flushing cycle (only when xanthan was injected)
- C1-C3** are flow rate controlled cycles
- C4** Pressure controlled step rate test



SEISMIC CHARACTERISTICS

Absolute location procedure:

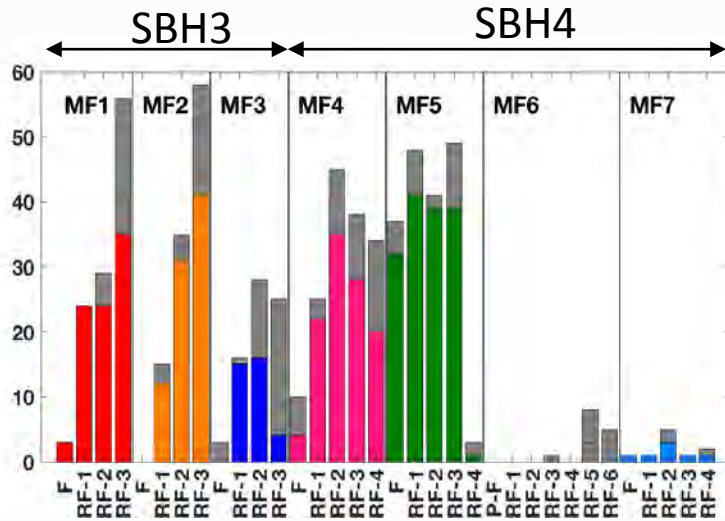
- Joint Hypocenter Determination (JHD)
- Velocity model: homogeneous, anisotropic
- Accuracy of location: ~ 0.5 m



- In total 6986 seismic events are recorded and 367 events are located.
- Seismicity clouds and plane fit to the localized seismic events for HF2, HF3 and HF8.

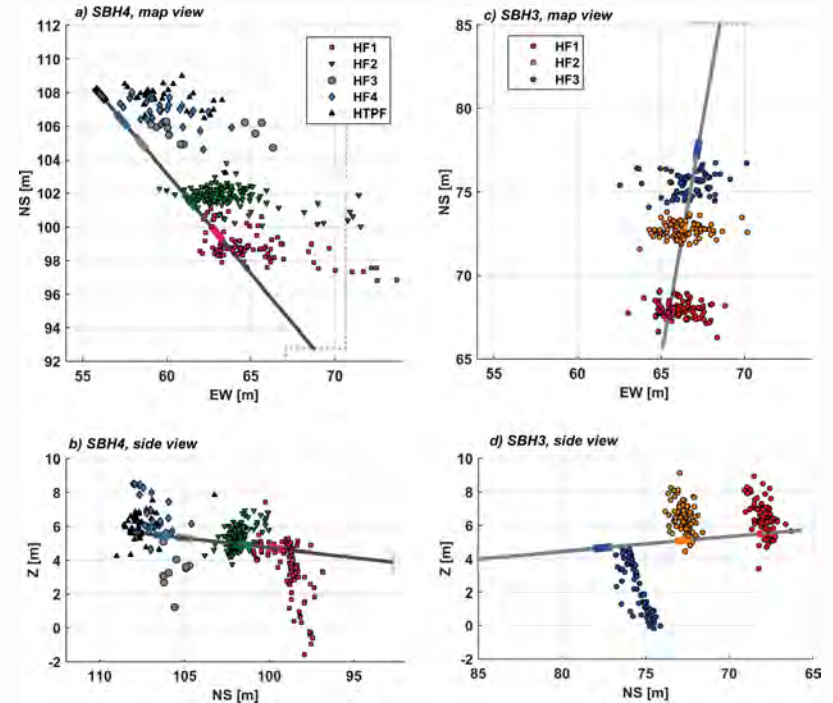
MINIFRACS FROM STRESS CHARACTERIZATION

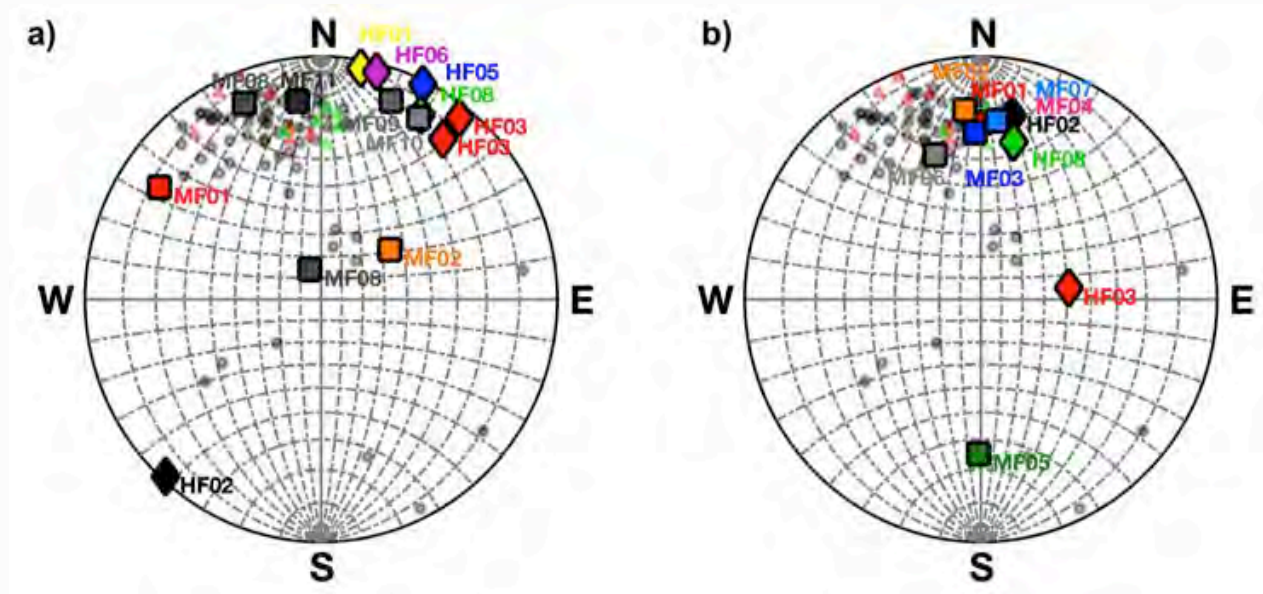
- MF1-MF3 location error < 2 m
- MF4-MF7 location error < 3 m
- The bars are colored if the event occurred during injection. The bar is grey during shut-in or bleed-off.



Gischig, V.S., et al., 2018, SE 9, 39–61.

Jalali, M., et al., 2018. Geophys. Res. Lett. 2017GL076781





The new created fracture traces from geophysical borehole logging and impression packer are presented in a lower hemisphere stereonet.

The plane fits from the seismic events are indicated in a lower hemisphere stereonet.

PENNY-SHAPED FLUID DRIVEN FRACTURE

– Definition of dimensionless toughness (Savitski & Detournay, 2002)

$$K = K' \times \left(\frac{t^2}{E'^3 \mu'^5 Q^3} \right)^{\frac{1}{18}}$$

Energy dissipation mechanism

$$K \leq 1$$

corresponds to the viscous fluid flow

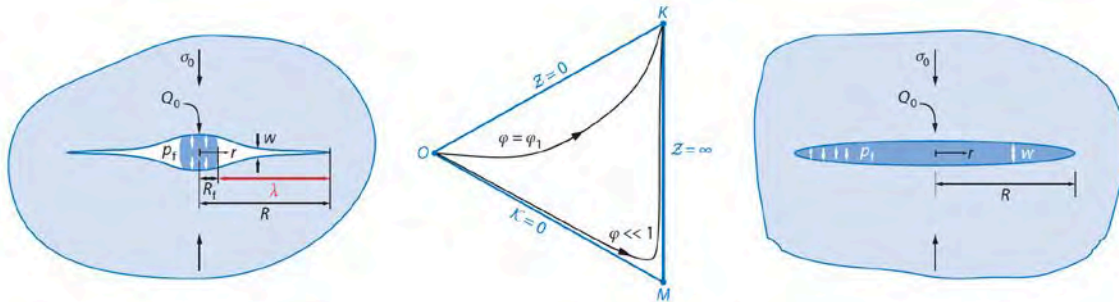
$$K \geq 3.5$$

corresponds to the creation of new surfaces

Vertex

M

K



Detournay, 2016

– Length asymptote for small (M) and large (K) time

$$L_m = \left(\frac{E' Q_0^3 t^4}{\mu'} \right)^{1/9}, \quad L_k = \left(\frac{Q_0 E' t}{K'} \right)^{2/5}.$$

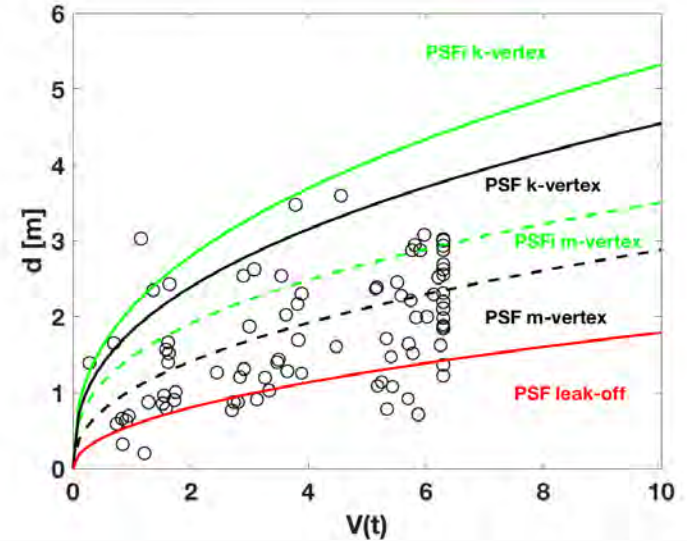
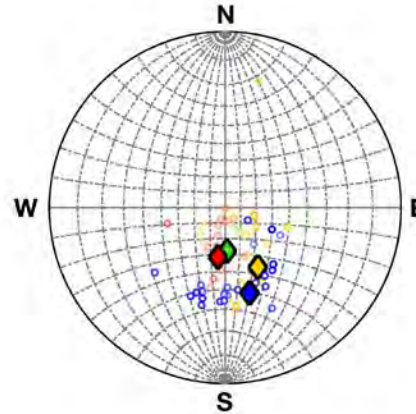
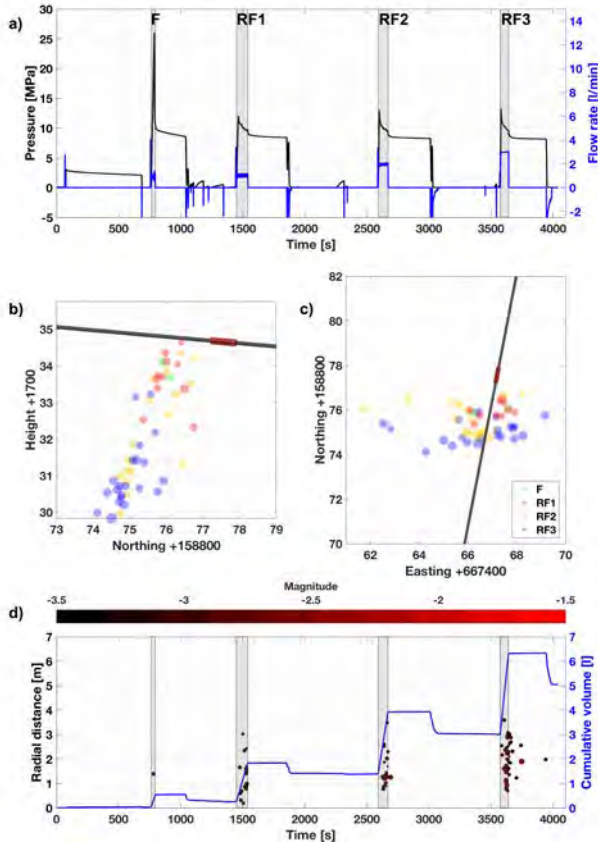
Equations to solve:

Elasticity

Lubrication approximation

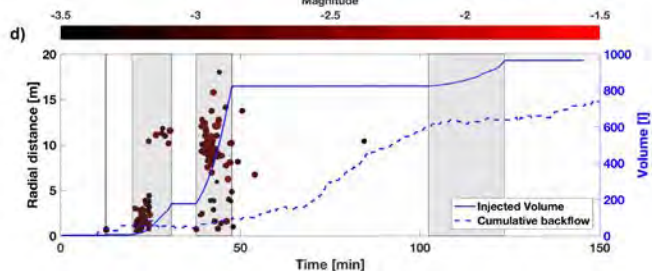
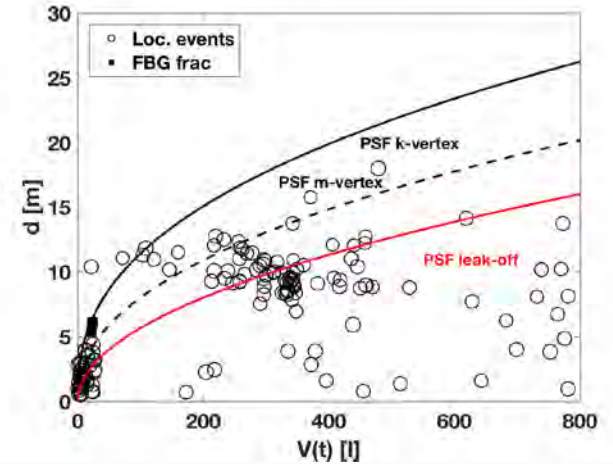
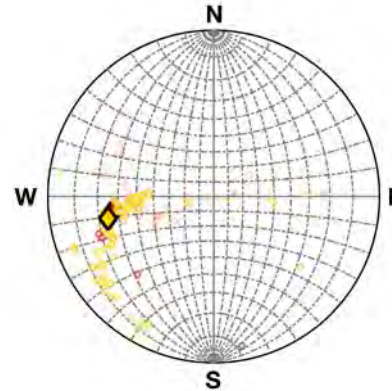
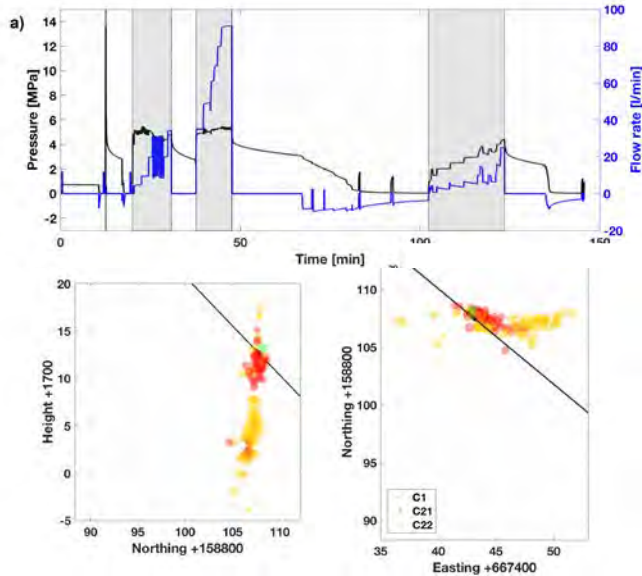
Boundary conditions

MF: COMPARING FRACTURE GROWTH OBSERVATIONS TO ANALYTICAL SOLUTIONS



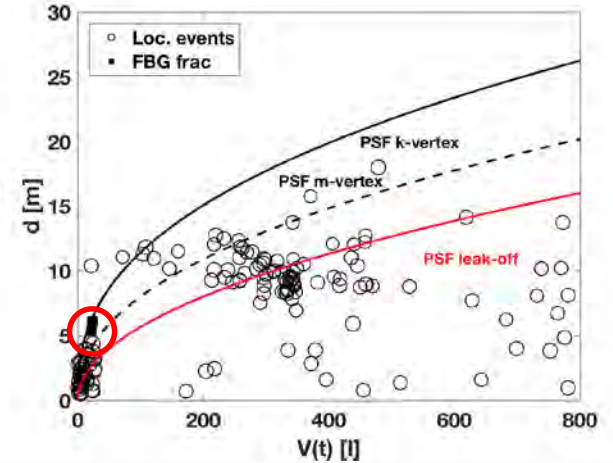
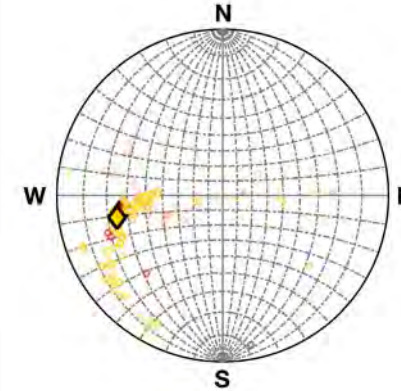
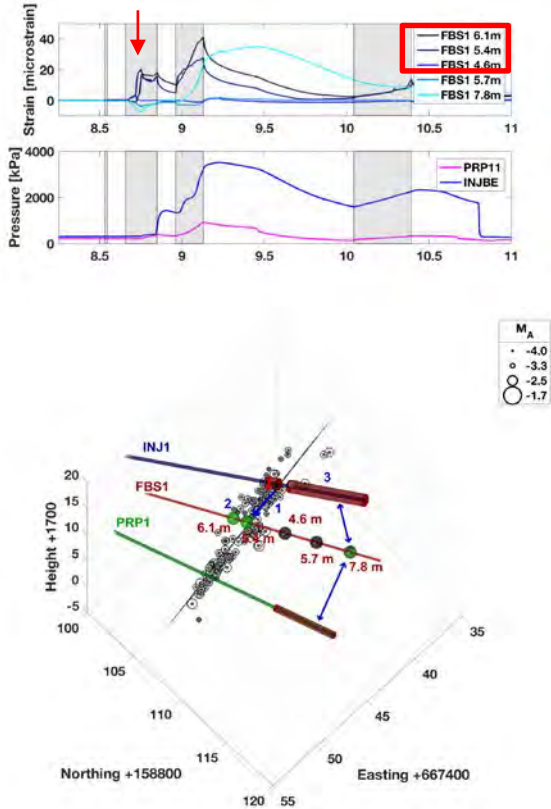
All events are located below the injection point and the fracture propagates downward. From the seismic cloud, only a partial penny-shaped fracture occur, whereby the error for small injection volumes is small.

HF: COMPARING FRACTURE GROWTH OBSERVATIONS TO ANALYTICAL SOLUTIONS



The fracture has a preferred seismic cloud growing downwards towards north. From the seismic cloud, only a partial penny-shaped fracture occur, whereby the error for small injection volumes is small. The error grows and it is necessary to account for permeable rock and leak-off.

HF: COMPARING FRACTURE GROWTH OBSERVATIONS TO ANALYTICAL SOLUTIONS



The fibre bragg grating (FBG) sensors are used to constrain the fracture geometry. Positive response indicate tension and negative response indicate compression.

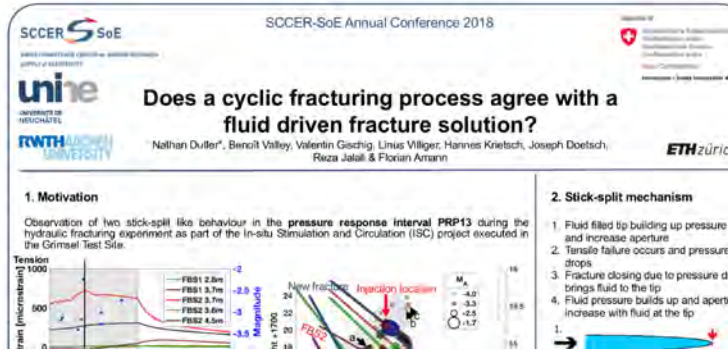
CONCLUSION

- The **seismic clouds indicate a preferential orientation** with a pole point towards sub-horizontal north (corresponds to minimum principal stress axis) and downwards in the HF experiment.
- The penny-shaped fracture geometry is able to reproduce the length of the minifrac. The **error of length increases due to the wrong approximation of the fracture geometry** with increasing fracture fluid volume. Changing the fracture geometry towards plane-strain is not an option, as this solution totally overestimate the fracture length.
- During the hydraulic fracturing experiment, seismic was observed up to 20 m away from the injection point. It seems, that network stimulation due to leak-off into pre-existing fractures takes over at early time.

THANK YOU FOR YOUR ATTENTION !

Poster:

Dutler Nathan, E215
Rue Emile Argand 11
CH-2000 Neuchâtel
nathan.dutler@unine.ch
www.unine.ch/chyn



REFERENCES

- Amann, F. et al, 2018. The seismo-hydromechanical behavior during deep geothermal reservoir stimulations: open questions tackled in a decameter-scale in situ stimulation experiment, *Solid Earth*, 9, 115-137, <https://doi.org/10.5194/se-9-115-2018>
- Detournay, E. (2016). Mechanics of Hydraulic Fractures. *Annual Review of Fluid Mechanics*, 48(1), 311–339. <https://doi.org/10.1146/annurev-fluid-010814-014736>
- Gischig, V.S., et al., 2018. On the link between stress field and small-scale hydraulic fracture growth in anisotropic rock derived from microseismicity. *Solid Earth* 9, 39–61.
- Jalali, M., et al., 2018. Transmissivity Changes and Microseismicity Induced by Small-Scale Hydraulic Fracturing Tests in Crystalline Rock. *Geophys. Res. Lett.* 2017GL076781
- Savitski, A. A., & Detournay, E. (2002). Propagation of a penny-shaped fluid-driven fracture in an impermeable rock: Asymptotic solutions. *International Journal of Solids and Structures*, 39(26), 6311–6337. [https://doi.org/10.1016/S0020-7683\(02\)00492-4](https://doi.org/10.1016/S0020-7683(02)00492-4)